

# FRACTURE CRITERIA FOR HYDROGEN AND TEMPER EMBRITTLEMENT IN 9Cr1Mo STEEL

M Wall, C E Lane and C A Hipsley\*

Stress and strain levels at fracture have been measured in 9Cr1Mo steel single-edge notched specimens subject to temper- and hydrogen-embrittlement. In contrast to some other studies of brittle fracture, the maximum stress attained in specimens at fracture was not found to be invariant with temperature. Careful analysis of initiation sites showed that the position of such sites relative to the stress/strain distribution was sensitive to temperature and embrittlement. The stress local to initiation sites was constant over the temperature range assessed. A dual stress/strain criteria model for brittle fracture is proposed which consistently predicts the behaviour of fracture parameters described. The observations are consistent with hydrogen reducing local fracture stress.

## INTRODUCTION

A reduction in ductility and toughness is observed on thermal ageing of 9Cr1Mo steels in the temperature range 400-650°C associated with intergranular phosphorus segregation and the precipitation of Laves phase ( $\text{Fe}_2\text{Mo}$ ) at the grain- and martensitic lath-boundaries. Hydrogen exacerbates this effect [1], and to investigate the mechanisms underlying this synergy, the effects of temper- and hydrogen embrittlement on stress and strain fracture parameters have been measured using single edge notched bend (SENB) specimens.

Results show that the peak stress ( $\sigma_F^*$ ) is not itself the controlling fracture parameter, but that its value is determined by satisfying local fracture conditions. The results have been analysed in terms of a dual criteria stress/strain model in which brittle fracture occurs as a dynamic event at a location where local

\* AEA Technology, Harwell Laboratory, OXON OX11 0RA, England

conditions for microcrack nucleation and propagation are satisfied simultaneously. The model is used to show that the primary effect of hydrogen is to reduce the cohesive strength associated with interfaces rather than to influence dislocation mobility.

### EXPERIMENTAL

A commercial cast of 9Cr1Mo steel was employed, with the following main constituents (wt%): C 0.11, Si 0.73, Mn 0.53, Cr 9.21, Mo 0.99, Ni 0.20. The alloy also contained 225wtppm P and 120wtppm S. SENB specimens with a 45° blunt notch/0.25mm root radius geometry were machined and heat treated to produce a normalised and tempered, fully martensitic microstructure (austenitisation 1100°C, 1h; normalise; temper 750°C, 1h). Batches of specimens were then aged at 550°C for 1000h and 5000h to produce temper embrittlement.

Specimens were tested in the unaged, 1000h and 5000h aged conditions, with and without hydrogen charging. Hydrogen was introduced to the SENB testpieces by electrolytic charging for 18h in 10% sulphuric acid + 1g/l thiourea (as a hydrogen recombination poison) at a current density of 5mA/cm<sup>2</sup>. This produced a bulk hydrogen content of 5-6wtppm in each specimen. The SENB samples were tested in four point bend over a range of temperatures between -196 and +50°C. Typical test duration was 20-30 minutes.

The load at fracture was determined from each test. This value was fed into a finite element elastic-plastic stress analysis for the SENB geometry, using tensile data previously derived, to produce the stress and strain distributions within the specimens at fracture. In this way, the maximum stress in the testpiece at fracture, commonly termed the 'microscopic cleavage fracture stress' could be derived i.e.  $\sigma_F^*$ . Each sample was then examined in the scanning electron microscope (SEM) to determine the location of microcrack initiation and the nature of the initiation site. The precise location of fracture initiation together with the finite element analysis enabled the actual principal stress and strain levels at the initiation site to be derived i.e.  $\sigma_{11c}$  and  $\epsilon_{11c}$  respectively.

### RESULTS

Figure 1 summarises the measurements of  $\sigma_F^*$  as a function of test temperature for all aged and hydrogen charged conditions. In this and subsequent figures these conditions are referred to as unaged, A1 (aged 1000h), A5 (aged 5000h), and +H (hydrogen charged). Clearly, in contrast to some other findings [2],  $\sigma_F^*$  does not

appear to be invariant with temperature, but decreases markedly as test temperature rises. This effect increases with the degree of embrittlement induced either by ageing or hydrogen or a combination of the two. Hydrogen has two further effects on  $\sigma_F^*$ : first, it tends to reduce the microscopic cleavage stress level for a given material condition; and secondly it extends the test temperature range over which brittle fracture conditions prevail i.e. the load at fracture is less than that required for general yield.

Fractographic examination showed that the fracture mode at initiation is dependent on temperature and hydrogen charging. At the lowest test temperatures, the fracture mode was predominantly transgranular cleavage (TC), and initiation occurred at inclusions or carbides. As the temperature rose, fracture became increasingly intergranular (IG) and the initiation sites were located within a group of intergranular facets. The same trend of rising tendency to IG fracture was observed with ageing and hydrogen charging, and the highest levels of IG fracture (70-80%) were found for 5000h aged material after hydrogen charging and testing at the highest temperatures, around ambient.

The location of the initiation sites also varies with temperature and hydrogen charging. A trend was observed in all material conditions, but particularly for the 5000h aged condition, in which the initiation site moves from close to the notch root towards the position of maximum stress ahead of the notch as temperature increases. This is illustrated in Figure 2, which plots the ratio of the distance of initiation sites ahead of the notch tip,  $X_c$ , to the distance of the maximum stress point ahead of the notch tip,  $X_p$ . Figure 2 also shows that charging with hydrogen generally pushed the initiation site towards the notch at equivalent temperatures.

Analysis of the principal stress and strain levels at crack initiation shows that, while  $\sigma_F^*$  fell with test temperature,  $\sigma_{11c}$  was effectively independent of temperature for a given condition. This is illustrated by Figure 3, which also shows that  $\sigma_{11c}$  was reduced by thermal ageing, and by hydrogen charging, the lowest values being observed for a combination of 5000h ageing and hydrogen charging.

#### DISCUSSION

The results presented above show that, for 9Cr1Mo steel in a variety of embrittled conditions,  $\sigma_F^*$ , the microscopic cleavage fracture stress, is not invariant with temperature, particularly when significant embrittlement, and hence intergranular fracture, is involved. This implies that the intergranular fracture process in this

material is not controlled solely by the attainment of a critical fracture stress. Most of the previous work on measurements of  $\sigma_F^*$  has focused on transgranular fracture [2], and shows that where this mode operates in isolation a simple critical fracture stress criterion can apply, and  $\sigma_F^*$  is invariant. Comparatively few studies of fracture involving the IG mode have been made, but in the few cases published [3] there is evidence to suggest that  $\sigma_F^*$  does indeed decrease as test temperature rises, consistent with the present data.

Thus the present study, together with some previous evidence, suggest that a more complex model of criteria for intergranular fracture is required. The critical fracture stress criterion is based on the assumption that microcrack initiation is relatively easy, and that fracture is controlled by the need to sustain conditions for crack propagation. Crack initiation occurs by the pile-up of dislocations against suitable initiation sites, such as inclusions, and is therefore plastic strain controlled, while crack propagation requires adequate stress levels in the material surrounding the nucleated microcrack.

The fact that nucleation occurs closer to the notch than the maximum stress point in many of the samples examined in this study suggests that crack nucleation is relatively difficult, requiring the higher levels of plastic strain to be found in these locations. We propose therefore a dual criteria model for intergranular fracture in which a critical stress for propagation and a critical strain for nucleation must be attained simultaneously. This situation is illustrated in Figure 4 in which the 'fracture zone', where cracks can both nucleate and propagate successfully, is a sub-set of regions satisfying individual critical stress and strain criteria. It is in this fracture zone, clearly between the notch tip and the maximum stress point, that the model would predict initiation sites to occur, as is in fact observed.

The validity of the dual criteria model can be assessed by its ability to account for the effects of temperature and embrittlement described above. As temperature rises, the stress and strain distributions broaden and more strain is required to reach a given level of stress. This makes the strain-controlled nucleation criterion relatively easy to satisfy, and the attainment of a critical stress tends to dominate the fracture zone. This in turn pushes the likely initiation site away from the notch tip towards the maximum stress point, as observed in Figure 3.

Current theories of hydrogen embrittlement attribute its effects either to a reduction in interfacial cohesion or to an influence on the nature of dislocation motion. The dual criteria model is consistent with the action of hydrogen in reducing grain-boundary cohesion and hence lowering the critical stress for crack propagation. If it is assumed that the strain criterion remains unchanged (i.e. the

same strain level is needed to nucleate microcracks), then as the critical fracture stress criterion falls, adequate stress levels will be attained at relatively lower loads, and the fracture zone will move towards the notch tip in order to satisfy the strain requirements. Figure 3 shows that, for a given test temperature, the effect of hydrogen is indeed to move the initiation site towards the notch tip, while Figure 2 confirms that the stress at fracture local to the initiation site is reduced in all material conditions by the presence of hydrogen.

### CONCLUSIONS

1. Hydrogen and thermal ageing both embrittle 9Cr1Mo steel, producing the most severe effect in combination. Embrittlement is associated with intergranular fracture.
2. Measurement of the maximum stress,  $\sigma_F^*$ , obtained in SENB samples at failure shows that  $\sigma_F^*$  decreases with test temperature, particularly for intergranular fracture, and hence that the fracture process is not controlled by  $\sigma_F^*$ .
3. The initiation sites for fracture were located between the notch root and the maximum stress point, moving towards the maximum stress point with increasing temperature and towards the notch root with increasing hydrogen embrittlement. The local stress at initiation was invariant with test temperature, but fell with both ageing and hydrogen embrittlement.
4. A dual criteria model for intergranular fracture is proposed in which critical levels of stress and strain must be satisfied simultaneously for a crack to nucleate and propagate successfully. This model can describe the effects of temperature on fracture behaviour described, and is consistent with the decohesion theory of hydrogen embrittlement.

### REFERENCES

- (1) Hippsley, C.A. and Haworth, N.P., Mater. Sci. Technol., Vol. 4, 1988, pp. 791-802.
- (2) Curry, D.A. and Knott, J.F., Met. Sci., Vol. 9, 1976, pp 390.
- (3) Ritchie, R.O., Genies L.C.E. and Knott, J.F., 3rd Conference on the Strength of Materials and Alloys, Cambridge, England, Institute of Metals, Vol. 1, 1973, pp 124-127.

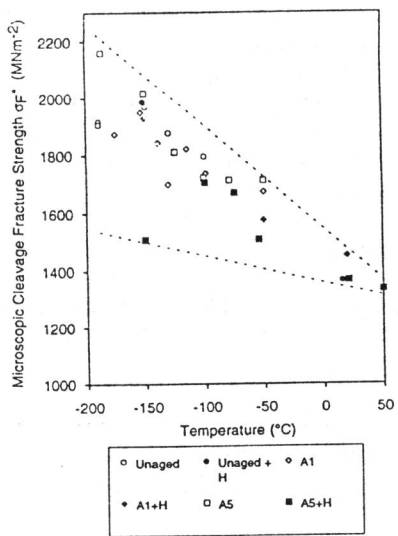


Figure 1 Peak tensile stress  $\sigma_F^*$  versus temperature

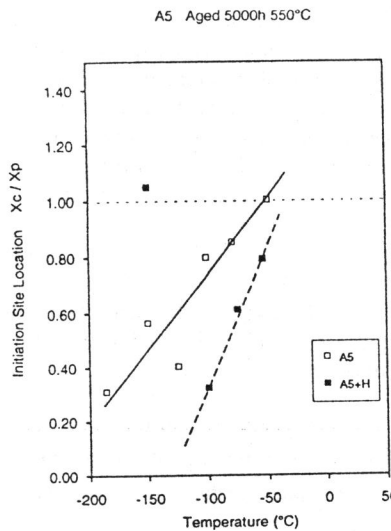


Figure 2 Initiation site location  $X_c$  relative to peak stress location  $X_p$

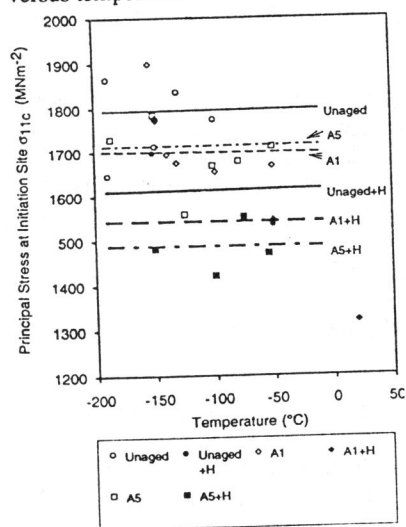


Figure 3 Principal stress at initiation site  $\sigma_{11c}$  versus temperature

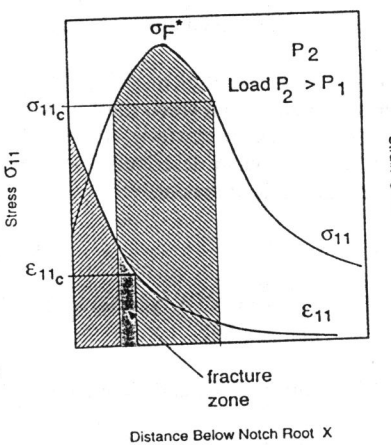


Figure 4 Schematic illustrating dual-criteria model for intergranular fracture